

Ferromagnetic stabilization of ordered B2 FeRh thin films

S. Lounis* and M. Benakki

Laboratoire de Physique et Chimie Quantique, Université Mouloud Mammeri, 15000 Tizi-Ouzou, Algeria

C. Demangeat

Institut de Physique et Chimie des Matériaux de Strasbourg, CNRS, 23, rue du Loess, F-67037 Strasbourg, France

(Received 3 September 2002; revised manuscript received 30 January 2003; published 31 March 2003)

The electronic structure and the local spin polarization of the (001) FeRh thin films have been studied within density-functional formalism. Bulk B2 FeRh is an ordered alloy, with in-plane antiferromagnetism (AF-II) in the Fe layers as ground state and a ferromagnetic configuration a few millirydberg above. A transition from antiferromagnetic to ferromagnetic configuration is obtained when the temperature is increased or when an excess of Fe is introduced. Here we demonstrate that a decrease of the film thickness leads to similar transition. For Rh-terminated FeRh (001) surfaces, the calculations show that the ground state of the film is ferromagnetic for nine layers whereas for 15 layers it is antiferromagnetic as in bulk FeRh.

DOI: 10.1103/PhysRevB.67.094432

PACS number(s): 75.70.Ak, 73.20.At, 75.50.Bb, 75.70.Rf

I. INTRODUCTION

Since the work of Fallot,¹ many detailed experimental studies have been made of the nearly equiatomic FeRh alloys. More recently, interest has focused on multilayers [FeRhIr/Ag/Fe (Ref. 2)] or epitaxial bilayers [Fe/FeRh(001) and NiFe/FeRh(001), (Ref. 3)] in order to explore different domain structures and exchange coupling leading to fascinating properties mainly induced by the magnetic transition from the antiferromagnetic ground state to the ferromagnetic one. Moruzzi and co-workers⁴⁻⁶ have used augmented spherical waves (ASW) method to study the binary FeRh ordered alloy. They investigated the following: (i) ferromagnetic configuration in which the Fe atoms polarize the neighboring Rh layers; (ii) layered antiferromagnetic configuration defined as ferromagnetic Fe planes separated by a nonmagnetic Rh plane, the Fe plane being antiferromagnetically coupled with its nearest-neighboring Fe planes (this magnetic configuration is called AF-I); (iii) in-plane antiferromagnetic configuration in each Fe plane (AF-II), the Rh atoms staying unpolarized. Their calculations reveal the coexistence of AF-II and FM solutions over a wide range of volume. The ground state is found to be AF-II with $\sim \pm 3\mu_B$ iron local moments and zero rhodium local moments in agreement with experimental values. The metastable ferromagnetic state with iron and rhodium local moments of $\sim 3.1\mu_B$ and $1\mu_B$ lies just above the AF-II state and has a minimum energy at a lattice constant $\sim 0.5\%$ larger than the AF-II state. AF-I is found at much greater energy.

The antiferromagnetic ground state of bulk FeRh can easily be changed to a ferromagnetic state due to elevated temperature whereby the phase transition is accompanied by a large drop in the electrical resistivity.⁷ The transition from the AF-II to the FM phase is very sensitive to heat treatment^{8,9} and magnetic field^{10,11}. The Curie temperature (T_C) and the transition from antiferromagnetic to the ferromagnetic state (T_{FM-AF}) are also very sensitive to chemical composition,^{12,13} the FM-AF transition being only present in

a very narrow concentration range of about 5% around $x = 0.5$ in the binary $\text{Fe}_{1-x}\text{Rh}_x$ phase diagram, and the ground state becomes ferromagnetic for $x = 0.51$.^{14,15} Attempts to elucidate the mechanism underlying the transition from AF-II to FM state were undertaken.¹⁶⁻¹⁹ Teraoka and Kanamori¹⁶ have extended the Anderson model of 3d virtual states. By taking an AF exchange interaction between Fe atoms and a FM exchange interaction between Fe and Rh atoms, they were able to show that the mechanism underlying the transition is an increase of the polarizability of the Rh atom and a decrease of the Fe-Fe exchange interaction with increasing temperature. Moriya and Usami¹⁷ have shown that the coexistence of ferromagnetism and antiferromagnetism, which breaks the symmetry, is possible in certain itinerant-electron systems where the wave-vector-dependent susceptibility neglecting the electron-electron interaction has two peaks at $q = 0$ and $q = Q$, the AF wave vector. For reasonable values of parameters within such a theory, they could explain the first-order transition in FeRh alloys. Hasegawa,¹⁸ using a tight-binding single band model and an intra-atomic electron-electron interaction, has determined the free energy within a spin-fluctuation theory. Hasegawa showed that by taking into account the effect of local spin fluctuations within the single site alloy analogy, a first-order transition takes place from one ordered state to a second ordered state. These models¹⁶⁻¹⁸ assumed a CsCl-type ordering of Fe and Rh atoms with equal concentration of Fe and Rh. Khan *et al.*¹⁹ examined the case of nonstoichiometry by considering only the $T = 0$ case. The aim is to produce evidence of a local mechanism which could be responsible for the nucleation of ferromagnetism in an AF FeRh alloy. To do that they replaced a Rh atom by an Fe atom in FeRh in its AF-II phase and looked for the effect of the nonstoichiometry on the magnetic behavior of the nearest neighbors of the substituted atom. Khan *et al.*¹⁹ within a semiempirical tight-binding formalism were able to display a spin flip of the Fe magnetic moments around an Fe impurity (equivalent to an excess of Fe in stoichiometric FeRh ordered alloys) substituting a Rh

atom. This shows clearly that a transition from zero magnetic moment towards a ferromagnetic surrounding can appear around an excess of Fe.

Within x-ray magnetic circular dichroism (XMCD) on $\text{Fe}_{0.51}\text{Rh}_{0.49}$, Chaboy *et al.*²⁰ confirmed the existence of a ferromagnetic ground state at low temperatures. Moreover they found the onset of two ferromagnetic phases located, respectively, below and above 150 K. Estimates of μ_{Rh} were obtained from the analysis of the XMCD data at the Rh $L_{2,3}$ edges, showing a depletion from $1.03\mu_B$ in the high-temperature ferromagnetic phase to $0.70\mu_{\text{Rh}}$ in the low-temperature one. This ferromagnetic-ferromagnetic transition is linked to a variation of volume of the sample. This can explain the large magnetovolumic effect observed in this system below $T=150$ K.²¹

The AF-FM transition of $\text{Fe}_x\text{Rh}_{1-x}$ was studied by van Driel *et al.*²² for film thicknesses up to 100 nm using x-ray-diffraction and Mössbauer spectroscopy. For $x_{\text{Fe}} < 0.5$, the amounts of the various crystallographically and magnetically distinct phases in the films were determined by conversion electron Mössbauer spectroscopy. In the composition range $0.4 < x_{\text{Fe}} < 0.5$, the observed transition temperature (from AF to FM) decreases down to 270 K. The decrease of the AF-FM transition temperature is explained by the stress present in the films²² and resulting from grain-to-grain or by compositional variations due to different amounts of excess Rh. Evidence of microstructural effects on this magnetic transition has been reported by Yokoyama *et al.*²³ who pointed out that the temperature interval in which the transition takes place increases with increasing grain size.

The purpose of this paper is to propose another mechanism for the stabilization of the ferromagnetic configuration in FeRh thin films and more precisely the possible stabilization of the ferromagnetic configuration when the thickness of the film decreases. This study follows directly previous study concerning the onset of AF configuration in thin bcc Fe films.²⁴ Following Kim and co-workers^{25,26} who obtained with quantitative low-energy electron diffraction an increase of the Rh concentration at the (110) surface of FeRh and the presence of 100% Rh at the first atomic layer of the (001) surface with 100% Fe at the second, we started our investigation by considering Rh at the (001) surface of FeRh. We also considered Fe at the surface but in that case no magnetic transition with the thickness of the film was obtained.

II. COMPUTATIONAL DETAILS AND MAGNETIC CONFIGURATIONS OF FeRh FILMS

All band-structure calculations presented here are based on scalar-relativistic version of the k -space tight-binding linear muffin-tin orbital method^{27,28} developed in the atomic spheres approximation. We perform the calculations with the Langreth-Mehl-Hu exchange-correlation term.²⁹ The equilibrium lattice parameters for bulk B2 FeRh alloys are determined by the minimization of the total-energy curve ($a = 5.62$ a.u. for AF-II and $a = 5.65$ a.u. for FM). The values obtained are in agreement with the calculations of Moruzzi and co-workers⁴⁻⁶ and the experimental measurements of Shirane *et al.*¹⁴ as it is shown in the Table I.

TABLE I. Comparison between the equilibrium lattice parameters (a) and magnetic moments (μ) of bulk B2 FeRh alloys obtained in the present calculation with those of another theoretical calculation and experimental measurements. Both AF-II and FM results have been reported. GGA stands for generalized gradient approximation, LSDA for local spin-density approximation.

	This work GGA ²⁹	ASW ⁴ LSDA ³²	expt. ¹⁴	Units
$a^{\text{AF-II}}$	5.62	5.647	5.639	a.u.
a^{FM}	5.65	5.673	5.667	a.u.
$\mu_{\text{Fe}}^{\text{AF-II}}$	3.11	2.980	3.3	μ_B
$\mu_{\text{Fe}}^{\text{FM}}$	3.188	3.15	2.8 ± 0.25	μ_B
$\mu_{\text{Rh}}^{\text{FM}}$	1.05	1.02	0.8 ± 0.25	μ_B

The films are modeled by repeated supercells made up by superposition of (i) alternative metallic monolayers of Fe and Rh (ii) empty layers. To cancel the interaction of two successive FeRh films, one separates them by a sufficient great number of empty spheres layers. This point is checked through vanishing charge in the central layer of the empty space and no dispersion along the Z -axis direction.³⁰ We have considered three well-known high-symmetry magnetic orders in Rh- and Fe-terminated (001) surfaces: the ferromagnetic configurations $P(1 \times 1)\uparrow$ and $P(1 \times 1)\downarrow$, and the $C(2 \times 2)$ in-plane antiferromagnetic configuration (a schematic representation of these magnetic configurations are reported in Fig. 1 of Elmouhssine *et al.*).³¹ One notices that for the AF-II phase, the $P(1 \times 1)\uparrow$ and $P(1 \times 1)\downarrow$ are equivalent. The electronic and magnetic structures are calculated using 121 k points in the first irreducible Brillouin zone.

We begin with a film thickness of nine atomic layers (AL) with an AF-II configuration and terminated by Rh. The $C(2 \times 2)$ order, in the surface, is characterized by non-magnetic Rh atoms at the layer surface (S) [Fig. 1(a)]. This is due (like in the bulk) to a magnetic frustration effect induced by the iron atoms that are coupled antiferromagnetically and situated at equal distance from the Rh atoms. It is clear that for this configuration, no surface effect is observed on the magnetism of Rh atoms at the S layer. Also the magnetic moments on the Fe atoms do not present significant changes. However, for $P(1 \times 1)\uparrow$ or $P(1 \times 1)\downarrow$ in the Rh surface layer a considerable modification of the magnetic map appears. On one hand, as seen in Fig. 1(b), only one self-consistent result is obtained. At the surface, the Rh atoms of the top layer have a moment of $1.08\mu_B$ close to the bulk FeRh value obtained in the ferromagnetic phase ($1.05\mu_B$). This value is also comparable to that ($0.82\mu_B$) calculated by Kachel *et al.*³³ in the case of a Rh monolayer deposited on Fe(001). On the other hand, one can notice a progressive decrease of the spin polarization on Rh atoms, from the surface layer S to the central layer of the film. The $S-2$ layer is characterized by a Rh moment of $0.55\mu_B/\text{atom}$ whereas, for the $S-4$ layer, the Rh polarization is $0.13\mu_B/\text{atom}$. The persistence of the Rh moment at the center of the slab shows the great effect of both surfaces and the magnetism induced by the Fe neighboring atoms situated at the subsurface layer. These Fe atoms

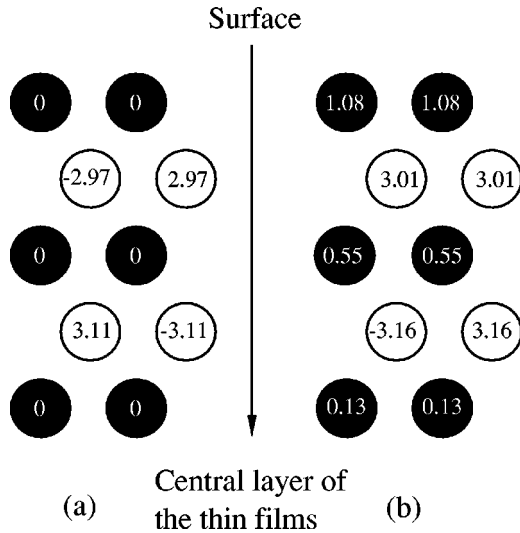


FIG. 1. Magnetic moments of the (001) FeRh films with 9 AL and AF-II magnetic configuration in the center, with Rh atoms in the top layer (dark circles) in a $C(2 \times 2)$ (a) and a ferromagnetic $P(1 \times 1)\uparrow$ (b) configurations. Starting with $P(1 \times 1)\downarrow$ leads to result (b).

present a ferromagnetic configuration with a moment of $3.01\mu_B$. A comparison between the energies shows that the most stable state is $P(1 \times 1)(\uparrow$ or $\downarrow)$. The difference in energy is 3.4 mRy/cell with the purely antiferromagnetic configuration (Table II). The magnetic coupling induced through the $P(1 \times 1)(\uparrow)$ configuration is definitively very different from the inner layers coupling and looks like a magnetic reconstruction at the surface. This result is interesting because it shows that a surface effect is able to stabilize a magnetic coupling at the surface layer (S) metastable in the bulk. The origin of this magnetic reconstruction may be due to the general ferromagnetic trend of the Rh when it grows on Fe substrates as studied by Kachel *et al.*³³ and by Zhong and Freeman.³⁴

In a second step, we start with FeRh films presenting a ferromagnetic coupling in the innerlayers of the slab. In the bulk, this ferromagnetic configuration is marginally less stable than the one with AF-II configuration. When the surface order is of $C(2 \times 2)$ type, the iron atoms of the subsurface layer have a moment of $\pm 3.05\mu_B$ [Fig. 2(a)]. Due to an

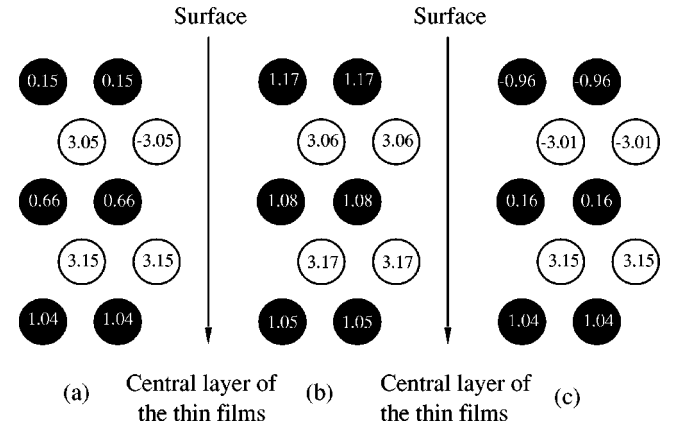


FIG. 2. Magnetic moments of the (001) FeRh films with 9 AL and FM configuration in the center, with Rh atoms in the top layer (dark circles) in a $C(2 \times 2)$ (a), a ferromagnetic $P(1 \times 1)\uparrow$ (b), an antiferromagnetic $P(1 \times 1)\downarrow$ (c) configurations.

antiferromagnetic coupling in the subsurface layer, one expects to obtain a zero moment for the Rh atoms at the surface layer arising from magnetic frustration effect. On the contrary one obtains a small spin polarization of the Rh atoms at the surface ($0.15\mu_B$). This polarization can be explained by two effects: surface effect and hybridization with both iron and rhodium atoms of the innerlayers. In contrast to the AF-II coupling case, there is an increase of the Rh magnetic moments when going from the surface to the inner layers i.e., $0.15\mu_B$, $0.66\mu_B$, and $1.04\mu_B$ for the layers S , $S-2$, and $S-4$.

The iron atoms of the subsurface layer for the $P(1 \times 1)\downarrow$ order have a moment of $-3.01\mu_B$ [Fig.2(c)]. As the magnetic coupling in this subsurface layer is ferromagnetic, this increases the magnetism of Rh at the surface S [as compared with the case with $C(2 \times 2)$ configuration], which reaches $-0.96\mu_B$. This value is, however, less than that obtained for the AF-II- $P(1 \times 1)\uparrow$ (or \downarrow) configuration. The Rh plane $S-2$ sandwiched between two antiferromagnetically coupled iron layers namely: $S-1$ and $S-3$, carry a moment of $0.16\mu_B$ per atom. The $P(1 \times 1)\uparrow$ order which corresponds to a continuity of the magnetic coupling of the inner layers is characterized by the the highest value of the Rh polarization at the surface S . The Rh moment reaches $1.17\mu_B$ [Fig. 2(b)] which is 11.4% higher than the bulk one. At the subsurface,

TABLE II. Difference ($E - E_0$) of energies (in millirydberg per cell) between FeRh films in terms of their number of atomic layers (9, 11, 13, and 15 AL), innerlayer couplings (AF-II, FM) and magnetic surface configurations [$C(2 \times 2)$, $P(1 \times 1)\uparrow$, $P(1 \times 1)\downarrow$] when Rh is a surface layer. E_0 is the energy of the most stable configuration.

Innerlayer couplings	Rh at the surface of FeRh thin films					
	AF-II			FM		
Surface (AL)	$C(2 \times 2)$	$P(1 \times 1)\uparrow$	$P(1 \times 1)\downarrow$	$C(2 \times 2)$	$P(1 \times 1)\uparrow$	$P(1 \times 1)\downarrow$
9	8.67	5.22	5.22	37.10	0	21.31
11	3.13	0.46	0.46	37.64	0	24.58
13	1.48	0	0		19.13	
15	1.15	0	0	48.34	12.66	36.72

the iron atoms have a moment of $3.06\mu_B$, whereas the S -3 layer carried a magnetic moment of $3.17\mu_B$. It is clear that at the surface, the high value of the Rh moment is most likely due to the broken symmetry which contracts the d band of the rhodium atoms (and thus increasing the density of states at the Fermi level) together with the strong hybridization arising from the ferromagnetic iron atoms. The Rh layer S -2 located between iron layers coupled ferromagnetically has a moment of $1.08\mu_B$ /atom.

The energetical comparison of the three magnetic orders at the surface shows that the $P(1\times 1)\uparrow$ configuration is the ground state (Table II). The energy difference between the $P(1\times 1)\uparrow$ order with, respectively, the $P(1\times 1)\downarrow$ and $C(2\times 2)$ orders is equal to 21.31 and 37.10 mRy/cell. Therefore, from Table II, we can say that the FeRh thin films with 9 AL and Rh surface layers are characterized by a FM- $P(1\times 1)\uparrow$ configuration which is more stable than AF-II- $P(1\times 1)\uparrow$ coupling in contrast with the bulk results. Thus for a thickness of 9 AL, the films are ferromagnetic and the difference in energy with the nearest metastable configuration is equal to 5.22 mRy/cell.

For thicknesses of 11 and 15 AL, the magnetic profiles are nearly the same than those obtained for a thickness of 9 AL. Therefore, we will not give a detailed description of the magnetic behavior but focus on their relative stability. For 11 and 15 AL with the AF-II phase in the inner layers, the most stable state is the $P(1\times 1)\uparrow$ that leads to a magnetic reconstruction as for 9 AL. However, one notices that there is a decrease of the difference in energy with the $C(2\times 2)$ order at the surface with the increase of the thickness of the films. Indeed, for 15 AL the difference diminishes down to 15% of the value obtained for 9 AL. For the two thicknesses with the FM coupling in the inner layers the same ground magnetic order at the surface, i.e., $P(1\times 1)\uparrow$ is also obtained. Having done that (Table II) we can display, in Fig. 3, the decrease of the difference in energy between the FM state (ground state for films with 9 and 11 AL) and the AF-II state stable for 15 AL (as well as in the bulk), versus film thicknesses. In the case of 13 AL we have encountered some convergency problems so that only two solutions are reported in Table II. Nevertheless, as in the case of 15 AL and bulk B2 FeRh alloys, this film remains clearly antiferromagnetic. It is clear that the induced polarization of the Rh atoms is able to stabilize the FM configuration in FeRh films with small thickness, but for greater thickness the gain of energy is not enough to destroy

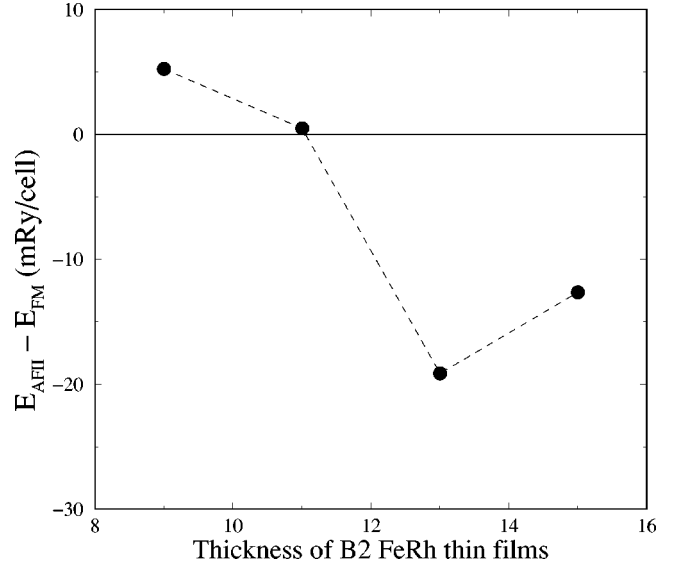


FIG. 3. Differences between AF-II and FM ground-state energies ($E_{AF-II} - E_{FM}$) (in millirydberg per cell) between FeRh films in terms of their thickness (9, 11, 13, 15 AL thick) when Rh is a surface layer.

the AF-II configuration. This is another way to stabilize the FM state, besides temperature effect and excess of Fe.

Finally, when Fe is at the top surface the ground state is the AF-II- $C(2\times 2)$ (Table III) for the three thicknesses considered (9, 11, and 13 AL). No magnetic reconstruction was observed.

III. CONCLUSION

In summary, we have shown that there is a clear correlation between the thickness of the FeRh thin films with Rh at the top layer and the stability of the magnetic configuration of the inner layers. Indeed the film with 9 AL is FM whereas the films with 13 and 15 AL remain AF-II like in the bulk, but the surface magnetic order does not show any drastic change with the film thickness. However, for Fe-terminated FeRh films such effect is not present. Therefore, one has to link this ferromagnetic stabilization of the films to the induced polarization of Rh resulting from both surface effect and induced polarization from ferromagnetic Fe. Indeed, as shown by Goldoni *et al.*³⁵ within linear magnetic dichroism

TABLE III. Difference ($E - E_0$) of energies (in millirydberg per cell) between FeRh films in terms of their atomic layers (9, 11, and 13 AL), innerlayer couplings (AF-II, FM) and magnetic surface configurations [$C(2\times 2)$, $P(1\times 1)\uparrow$, $P(1\times 1)\downarrow$] when Fe is a surface layer. E_0 is the energy of the most stable configuration.

Innerlayer couplings Surface (AL)	Fe at the surface of FeRh thin films					
	$C(2\times 2)$	AF-II		$C(2\times 2)$	FM	
		$P(1\times 1)\uparrow$	$P(1\times 1)\downarrow$		$P(1\times 1)\uparrow$	$P(1\times 1)\downarrow$
9	0.00	0.11	0.11	50.16	20.55	23.41
11	0.00	1.16	1.16	58.63	23.48	26.71
13	0.00	0.83	0.83	65.43	31.96	34.35

in angular distribution, the surface of Rh(100) is not ferromagnetic. Therefore, surface effect alone cannot induce a magnetic moment. Sizable polarization can only arise by contact with an Fe ferromagnet.^{33,36} As seen in Fig. 2(b), an increase of Rh polarization (from $1.05\mu_B$ in the bulk FeRh to $1.17\mu_B$ at the surface) is able to stabilize the FM configuration. This cannot happen with Fe at the surface, since the moment of Fe in bulk FeRh is already very high so that an increase is almost unlikely.

ACKNOWLEDGMENTS

This work was supported partly by Algerian Project ANDRU/PNR3 (Grant No. AU 49902) and by a collaborative program 99 MDU 449 between University Louis Pasteur of Strasbourg, France and the University Mouloud Mammeri of Tizi-Ouzou, Algeria. Institut de Physique et Chimie des Matériaux de Strasbourg is Unité Mixte de Recherche 7504 between CNRS and University Louis Pasteur.

*Corresponding author. FAX: 00 (213) 26 21 48 48. Email address: samir_lounis@yahoo.fr

¹M. Fallot, Ann. Phys. (Paris) **10**, 291 (1938).

²S. Hashi, M. Inoue, K.I. Arai, and Y.S. Kim, J. Appl. Phys. **85**, 6241 (1999).

³S. Yuasa, M. Nývlt, T. Katayama, and Y. Suzuki, J. Appl. Phys. **83**, 6813 (1998).

⁴V.L. Moruzzi and P.M. Marcus, Phys. Rev. B **46**, 2864 (1992).

⁵V.L. Moruzzi and P.M. Marcus, Phys. Rev. B **48**, 16 106 (1993).

⁶P.M. Marcus, V.L. Moruzzi, and S.L. Qiu, Phys. Rev. B **54**, 11933 (1996).

⁷J.S. Kouvel and C.C. Hartelius, J. Appl. Phys. **33**, 1343 (1962).

⁸M. Takahashi and R. Oshima, Mater. Trans., JIM **36**, 735 (1995).

⁹J.M. Lommel and J.S. Kouvel, J. Appl. Phys. **38**, 1263 (1967).

¹⁰J.B. Mckinnon, D. Melville, and E.W. Lee, J. Phys. C **3**, S46 (1970).

¹¹B.K. Ponomorev, Sov. Phys. JETP **36**, 105 (1973).

¹²E.M. Hofer and P. Cucka, J. Phys. Chem. Solids **27**, 1552 (1966).

¹³N.I. Kulikov, E.T. Kulatov, L.I. Vunokurova, and M. Pardavi-Horvath, J. Phys. F: Met. Phys. **12**, L91 (1982).

¹⁴G. Shirane, C.W. Chen, P.A. Flinn, and R. Nathans, Phys. Rev. **131**, 183 (1963); G. Shirane, R. Nathans, and C.W. Chen, *ibid.* **134**, 1547 (1964).

¹⁵P. Tu, J. Heeger, J.S. Kouvel, and J.B. Comly, J. Appl. Phys. **40**, 1368 (1969).

¹⁶Y. Teraoka, and J. Kanamori, Physica B & C **91**, 199 (1977).

¹⁷T. Moriya and K. Usami, Solid State Commun. **23**, 935 (1977).

¹⁸H. Hasegawa, J. Phys. Soc. Jpn. **49**, 178 (1980).

¹⁹M.A. Khan, Y. Khwaja, and C. Demangeat, J. Phys. (Paris) **42**, 573 (1981).

²⁰J. Chaboy, F. Bartolomé, M.R. Ibarra, C.I. Marquina, P.A. Algarabel, A. Rogalev, and C. Neumann, Phys. Rev. B **59**, 3306 (1999).

²¹M.R. Ibarra and P.A. Algarabel, Phys. Rev. B **50**, 4196 (1994).

²²J. van Driel, R. Coehoorn, G.J. Strijkers, E. Brück, and F.R. de Boer, J. Appl. Phys. **85**, 1026 (1999).

²³Y. Yokoyama, M. Usukura, S. Yuasa, Y. Suzuki, H. Miyajima, and T. Katayama, J. Magn. Magn. Mater. **177–181**, 181 (1998).

²⁴H. Nait-Laziz and C. Demangeat, Appl. Surf. Sci. **65–66**, 165 (1993).

²⁵S.K. Kim, Y. Tian, F. Jona, and P.M. Marcus, Phys. Rev. B **56**, 9858 (1997).

²⁶S.K. Kim and F. Jona, Surf. Rev. Lett. **7**, 115 (2000).

²⁷O.K. Andersen, Phys. Rev. B **12**, 3060 (1975).

²⁸O.K. Andersen and O. Jepsen, Phys. Rev. Lett. **53**, 2571 (1984).

²⁹D.C. Langreth and M.J. Mehl, Phys. Rev. Lett. **47**, 446 (1981); C.D. Hu and D.C. Langreth, Physica C **32**, 391 (1985).

³⁰M.A. Khan, J. Phys. Soc. Jpn. **62**, 1682 (1993).

³¹O. Elmouhssine, G. Moraitis, C. Demangeat, and J.C. Parlebas, Phys. Rev. B **55**, R7410 (1997).

³²L. Hedin and B.I. Lundqvist, J. Phys. C **4**, 2064 (1971); U. von Barth and L. Hedin, *ibid.* **5**, 1629 (1972).

³³T. Kachel, W. Gudat, C. Carbone, E. Vescovo, S. Blügel, U. Alkemper, and W. Eberhardt, Phys. Rev. B **46**, 12 888 (1992).

³⁴L. Zhong and A.J. Freeman, J. Appl. Phys. **81**, 3890 (1997).

³⁵A. Goldoni, A. Baraldi, M. Barnaba, G. Comelli, S. Lizzit, and G. Paolucci, Surf. Sci. **454–456**, 925 (2000).

³⁶A. Chouairi, H. Dreyssé, H. Nait-Laziz, and C. Demangeat, Phys. Rev. B **48**, 7735 (1993).